

# Neutrino Signals in IceCube from Weak Production of Top and Charm

Vernon Barger<sup>1</sup>, Edward Basso<sup>1</sup>, Yu Gao<sup>2,3</sup>, and Wai-Yee Keung<sup>4</sup>

<sup>1</sup>*Department of Physics, University of Wisconsin,  
Madison, WI 53706, USA*

<sup>2</sup>*Mitchell Institute for Fundamental Physics and Astronomy,  
Texas A&M University,  
College Station, TX 77843-4242, USA*

<sup>3</sup>*Department of Physics and Astronomy,  
Wayne State University, Detroit, MI, 48201 USA*

<sup>4</sup>*Physics Department,  
University of Illinois at Chicago, IL 60607*

Deep inelastic scattering of very high-energy neutrinos can potentially be enhanced by the production of a single top quark or charm quark via the interaction of a virtual  $W$ -boson exchange with a  $b$ -quark or  $s$ -quark parton in the nucleon. The single top contribution shows a sharp rise at neutrino energies above 0.5 PeV and gives a cross-section contribution of order 5 percent at 10 PeV, while single charm has a low energy threshold and contributes about 25 percent. Semi-leptonic decays of top and charm give di-muon events whose kinematic characteristics are shown. The angular separation of the di-muons from heavy quark production in the IceCube detector can reach up to one degree. Top quark production has a unique, but rare, three muon signal.

## I. INTRODUCTION

The ultra-high energy cross-section for neutrino deep inelastic scattering (DIS) has long been of theoretical interest. See, e.g.[1]. The DIS cross-section contributions due to the  $b$ -quark to  $t$ -quark transition and the  $s$ -quark to  $c$ -quark transition, mediated by  $W$ -boson exchange[2], may be observable in the IceCube experiment. With the recently improved determinations of the  $b$ -quark and the  $s$ -quark parton distributions function (PDFs), single top-quark and single charm-quark production by neutrinos can be calculated with a high degree of confidence and this is one objective of our study.

The IceCube experiment has recently reported results from 7 years of data[3]. Neutrino events with energies in the range 240 TeV to 10 PeV are found at a level that significantly exceeds the atmospheric neutrino background which is steeply falling with increasing energy. These observations have sparked interest in possible origins of the high energy events [4], including astrophysics sources, such as AGN and star-burst galaxies [5], or new physics, such as leptoquarks [6–8] and the decays of very-long-lived neutral particles associated with quasi-stable dark matter[9–12].

The Standard Model contributions from the production of a single top-quark and a single charm-quark will enhance the DIS neutrino cross at PeV-energies and thus these contributions are relevant to IceCube observations. We evaluate their DIS contributions and consider the characteristics of di-muon events associated with the semi-leptonic decays of the  $t$ -quark and  $c$ -quark.

We begin with a brief overview of the IceCube experiment and datasets. IceCube is a 1 km<sup>3</sup> photomultiplier-instrumented detector located in the South Pole ice sheet. The detector measures the total Cherenkov light emission in a high-energy neutrino event. The produced leptons

and hadrons contribute to the observed Cherenkov light. The IceTop array of ice tanks on the surface is used to detect and reconstruct air showers; it thereby vetoes the large cosmic muon backgrounds.

There are two classes of events:

1) “Track-like” events are those with a highly energetic muon produced in the interaction of a  $\nu_\mu$  within the detector or in the surrounding ice or rock. In addition to rejection of cosmic muon backgrounds by IceTop, the Earth also serves as a filter to eliminate cosmic muon backgrounds. Muons with arrival directions above 85 degrees in zenith angle must originate from neutrino interactions, even if the muon track originates outside the detector volume.

2) “Shower-like” events are those with an electromagnetic shower that is contained in the detector but there is no muon track. These events are due to  $\nu_e$  or  $\nu_\tau$  charged-current events, as well as neutral current events, though the neutral current contributions are sub-dominant.

The Class 1 track events are up-going in the detector. They are essentially free of the atmospheric background, but they provide only partial sky coverage. There is a significant loss of the very high energy neutrino flux in the propagation of the neutrinos through the Earth.

The Class 2 shower events are required to have the visible electromagnetic energy confined within the detector volume. The cosmic muon background is rejected by IceTop. The Class 2 events have full sky coverage.

The contributions to the atmospheric neutrino flux from pair-production of charm particles by the strong interaction have been considered [13–16], with the conclusion that this source cannot explain the excess of events observed by IceCube above 30 TeV[14].

In the Class 1 track events, the most probable neutrino energy cannot be precisely determined because the high-energy muon often passes through and exits the detector.

However, the neutrino direction of the track events is well determined to less than 0.5 degree.

In the Class 2 shower events, the energy of the incident neutrino is reasonably well determined, while the neutrino direction has large uncertainty (with a median uncertainty of 10 degrees).

Thus, the two Classes of events are complementary in their physics information. In both Classes, the neutrino energy dependence is steeply falling up to 100 TeV, as expected from the flux of atmospheric neutrinos. Above 240 TeV, the neutrino flux has a flatter energy spectrum that is consistent with a  $E_\nu^{-2}$  power law, typical of an astrophysics Fermi acceleration mechanism of cosmic rays [17]. Whether there is a maximum energy cut-off of the neutrino flux remains an open question.

The three most energetic shower events have energies of 1.041 PeV, 1.141 PeV and 2.0 PeV, with 15% energy resolution. A track event was found with an exceptionally high-energy muon with  $2.6 \pm 0.3$  PeV deposited energy. These are the highest energy neutrinos ever recorded by any experiment. The high-energy neutrino flux inferred by IceCube depends on the effective area of the detector under the assumption that the neutrino inclusive cross-section can be accurately modeled by charged-current and neutral-current DIS on light-quark flavors. Our study evaluates the impact of the  $b$ -quark to  $t$ -quark and the  $s$ -quark to  $c$ -quark transitions, treating the  $b$ -quark as a massless parton in the proton [18, 19] in the 5-flavor formalism. In addition, we simulate the muon distributions in di-muon events for a further probe of heavy quark contributions. Our focus is on events in which the deep inelastic interaction on a proton target of a  $\nu_\mu$  gives a fast primary muon.

## II. SLOW SCALING IN TOP-QUARK PRODUCTION

In a 4-flavor parton scheme (4FS), the leading-order (LO) partonic process for the QCD production of a  $b$ -quark is  $gluon$  to  $b\bar{b}$  and the top-quark is produced from the  $b$ -quark in an overall 2 to 3 particle process. In the 4FS, the integration over the final-state bottom-quark momenta leads to logarithmic dependence on  $m_b$ . In a 5-flavor scheme (5FS), these logarithms are re-summed to all orders in the strong coupling into a  $b$ -quark parton distribution function (PDF).

In the 5FS, the  $b$ -quark mass is set to zero, and all collinear divergences are absorbed into the PDF through mass factorization. The dependence on the  $b$ -quark mass is encoded as a boundary condition on the Renormalization Group Equations. In the 5FS, top-production in DIS is a 2 to 2 particle process. We adopt the 5FS for our calculations for effectiveness, since either the 4FS or 5FS scheme should give the same cross-section. [20] A similar use of the  $b$ -parton PDF in the calculation of Higgs production at colliders can be found in [20, 21].

The leading order Feynman diagram for top-quark pro-

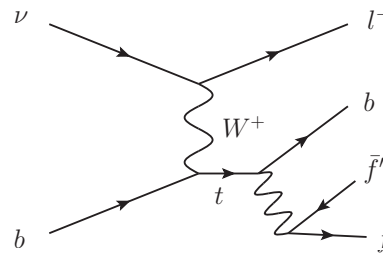


FIG. 1: Leading order Feynman diagram for neutrino production of the  $t$ -quark from the  $b$ -quark parton in the nucleon,  $\nu b \rightarrow lt$ . The  $W$ -boson decays to a fermion and an anti-fermion

duction in the 5FS via the weak charged-current neutrino interaction is shown in Fig. 1, along with the top-quark decay to a  $b$ -quark and a real  $W$ -boson.

The charged current subprocess  $\nu b \rightarrow lt$  gives the deep inelastic  $t$ -quark production cross-section. In the excellent approximation that the quark mixing matrix element  $V_{tb} = 1$ , the differential DIS cross section is given by

$$\frac{d\sigma}{dx dy} = \frac{G_F^2 (\hat{s} - m_t^2) m_W^4}{\pi(Q^2 + m_W^2)^2} b(x', \mu^2), \quad (1)$$

where the momentum transfer  $q = p_\nu - p_\ell$  sets the scale  $Q^2 = -q^2 > 0$ . The Bjorken scaling variables are  $x = Q^2/2p \cdot q$  and  $y = p_N \cdot q/m_N$ ,  $Q^2 = sxy$ , and  $y = (E_\nu - E_\ell)/E_\nu = E_h/E_\nu$  is the fraction of the neutrino energy that is transferred to hadrons. The CM energy squared of  $\nu N$  scattering is  $s = 2m_N E_\nu$ , neglecting the small  $m_N^2$  contribution. From kinematics, the fractional momentum of the  $b$ -parton is  $x' = x + m_t^2/ys$ . The subprocess CM energy squared is  $\hat{s} = (p_\nu + p_b)^2 = x's$ . The domains of the  $x, y$  variables are

$$m_t^2/s < y < 1 \quad \text{and} \quad 0 < x < 1 - \frac{m_t^2}{sy}. \quad (2)$$

Note that  $b(x', \mu^2)$  is evaluated at the slow scaling variable, i.e.  $x'$ .

After variable substitutions, we also obtain the formula

$$\frac{d\sigma}{dx dy} = \frac{G_F^2 (2m_N E_\nu x + m_t^2/y - m_t^2) m_W^4}{\pi(m_W^2 + 2m_N E_\nu xy)^2} b\left(x + \frac{m_t^2}{sy}, \mu^2\right), \quad (3)$$

with  $y(1-x) > m_t^2/s$ . Note that the numerator factor  $(xs + m_t^2/y - m_t^2) \rightarrow xs$  when  $\hat{s} \gg m_t^2$ , and thus  $xb(x)$  is obtained in Eq. (3) well above threshold. A similar formula applies to the anti-neutrino case. In our calculations we take  $m_t$  for both factorization and renormalization scales, as found in other applications to reproduce NLO and NNLO results in a LO calculation[20, 21]

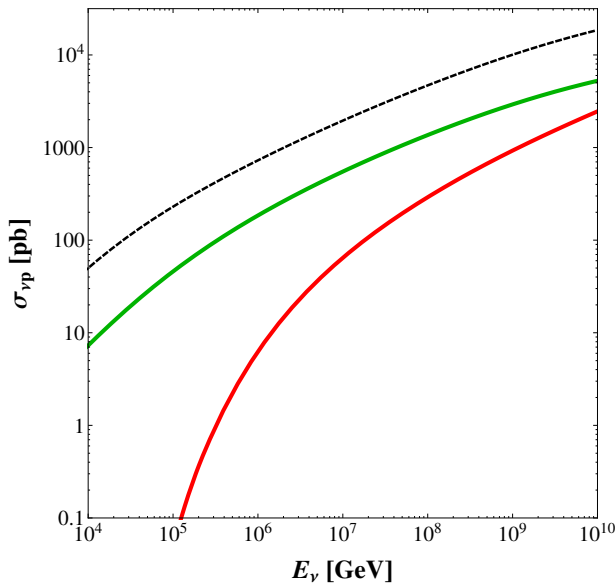


FIG. 2: Deep-inelastic  $\nu_\mu$  cross-section for charged-current scattering on a proton target. The upper curve is the standard result for  $u, d, s, c$  partons. The bottom curve is the DIS contribution from scattering on the  $b$ -quark parton to produce the  $t$ -quark. The middle curve shows the cross-section from the  $s$ -quark to  $c$ -quark process.

### III. CROSS SECTIONS AND $y$ -DISTRIBUTIONS

The calculated neutrino DIS charged-current cross sections are shown in Fig. 2 versus the neutrino energy. The upper curve is the result for 4 light parton flavors ( $u, d, s, c$ ), including NLO QCD corrections[22] which are found to be -1% of the LO result at all energies and thus are insignificant. However, the calculated DIS cross sections are subject to possible overall uncertainties associated with the PDFs, but again these will be independent of neutrino energy. The lower curve in Fig. 2 is the contribution from top-quark production. Above 10 PeV the top-quark cross section approaches 5 percent of the usual CC result. The middle curve is the contribution from  $c$ -quark production from the  $s$ -quark. Single charm production is about 25 percent of the total DIS. The weak production of the charm quark from the strange quark in the proton has a low neutrino energy threshold and the energy dependence is quite unlike the steep rise with energy of top quark production.

Physics with a high threshold energy, like the top, will first become evident at low  $x$  and high  $y$ . The distributions in the scaling variable  $y = 1 - E_\mu/E_\nu$  are shown in Fig. 3a, for three choices of neutrino energy: 0.1 PeV (close to the threshold for top production), 1 PeV (an energy for which the background from atmospheric neutrinos is negligible) and 10 PeV (where the  $y$ -distribution for top production approaches the shape of the usual result of 4-quark flavors). The  $y$ -distribution at 0.1 PeV clearly exhibits the kinematic suppression from the top-

quark threshold.

The theoretical distribution in the  $y$  variable from scattering on light partons has been used by the IceCube collaboration in estimating the neutrino energy of through-going muon events from the Cherenkov light. Figure 3b compares the average- $y$  values,  $\langle y \rangle$ , for production from 4-quark flavors with that from top-production. There are substantial differences in  $\langle y \rangle$  for neutrino energies of 1-10 PeV. Thus, since  $E_\nu = E_{\text{hadron}}/y$ , a higher neutrino energy would be inferred for an event assuming production from light partons then would be the case if it is a top-quark event. However, the importance of this effect should be modest, since the top cross section at a neutrino energy of 1 PeV is only at the 5 percent level. At the highest energies in Fig. 3b, the 4-flavor and  $t$ -quark results for  $\langle y \rangle$  converge, since sea quarks then dominate the cross sections. We note that the trend towards smaller  $y$  with increasing energy, for both the usual CC and  $t$ -quark cross-sections, is a consequence of the  $Q^2$  dependence of the  $W$ -propagator, which suppresses high- $y$  contributions.

### IV. DI-MUON EVENTS

In addition to a primary muon in the DIS of  $\nu_\mu s$ , the decays of a top quark into  $B$ -mesons or of a charm quark into  $D$ -mesons will lead to additional muons in about 10 percent of heavy quark events. In the following we label the most energetic muon in an event as  $\mu_1$ , which mostly will be the primary muon from the neutrino production vertex and that of the second most energetic muon as  $\mu_2$ , which will mostly be the muon from the decay of the heavy quark.

At high neutrino energies,  $\mu_2$  will typically also have high energy due to large Lorentz boost from the center-of mass frame to the laboratory frame. We simulate the predicted kinematic distributions of these muons from heavy quark decays using MadGraph5 [23] for the production cross sections and PYTHIA6 [24] for the hadronizations into  $B$  and  $D$  mesons as well as their decays. Top quarks decay before hadronization, so we include the spin correlations of production and decay in that case.

The muon energy distributions are shown in Fig. 4 and the angular separations of the two leading (in energy) muons are shown in Fig. 5, at an incoming neutrino energy of 1 PeV. In each figure,  $\nu b$  represents a  $b$  to  $t$  conversion,  $\nu s$  represents  $s$  to  $c$  conversion, etc. All muons in the final state, both from the neutrino-vertex and those from a real  $W$ -boson, when present, and the  $B, D$  decays, are included. The muons from decays of the longer lived pions and kaons are not included as they will lose energy quickly and range out during their propagation in the ice or rock.

The corresponding distributions from  $\nu_e$  DIS are shown in Fig. 4 as a useful comparison.  $\mu_1$  of an  $\nu_e$  event has the energy distribution of  $\mu_2$  in a  $\nu_\mu$  event. The energy of the fastest muon is required to exceed 0.5 PeV in these

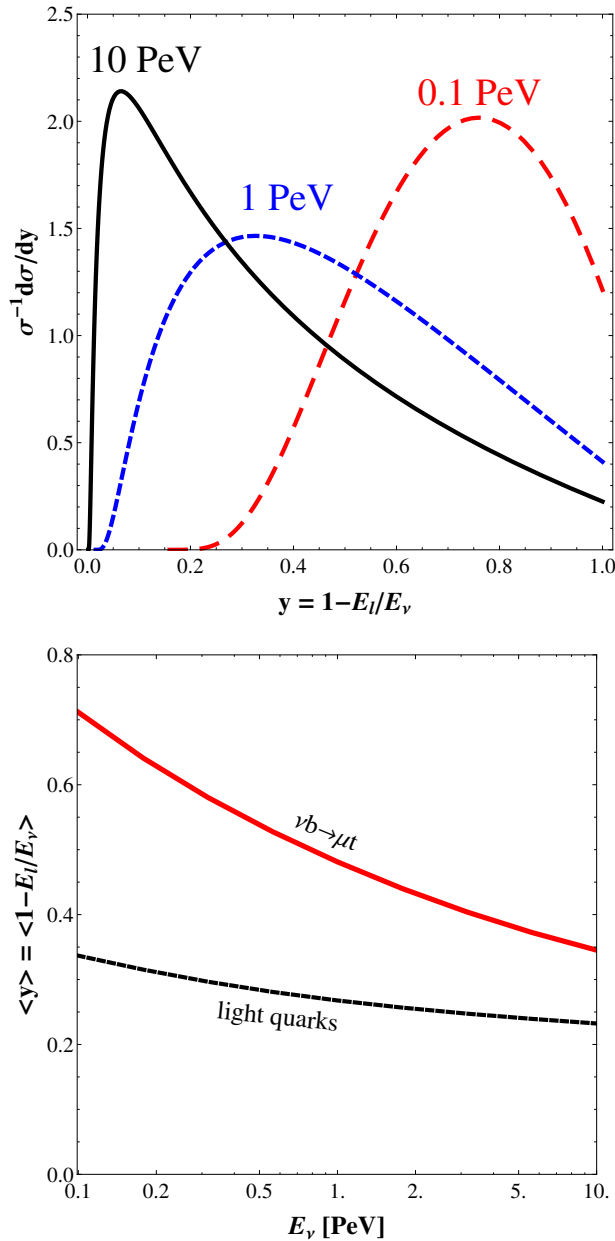


FIG. 3: (a) Distributions versus the scaling variable  $y = 1 - E_l/E_\nu$  in charged-current neutrino deep-inelastic scattering, at neutrino energies of 0.1, 1, and 10 PeV; the distributions are normalized to unity to facilitate comparison of the shapes; (b) Average  $y$  versus neutrino energy for scattering on  $u, d, s$  and  $c$  (dashed curve) and for scattering on the  $b$ -quark parton to produce the  $t$ -quark (solid curve).

plots. For  $\nu_e$  DIS, 46 percent of  $b$  to  $t$  and 11 percent of  $s$  to  $c$  satisfy this energy requirement.

The observation of an energetic  $\mu_2$  will signal a heavy quark event. The charm contribution dominates over top by about a factor of 10 for a 1 PeV primary neutrino energy, so disentangling the top signal from energy distributions alone would be challenging, but the angular separation of the two muons is more favorable, as

discussed below. The proposed Generation 2 expansion of the IceCube detector yield a factor of 10 increase in events, along with sensitivity to higher neutrino energies, which may make a partial distinction possible of the di-muon signals from top and charm.

Due to the very small deflection angle of a primary muon from the neutrino direction, the  $P_T$  of  $\mu_2$  with respect to the neutrino is essentially the same as relative to the  $\mu_1$  direction. In  $\nu_e$  events both muons originate from the hadron vertex and consequently the  $P_T$  distribution is much softer, as can be seen in Fig. 4.

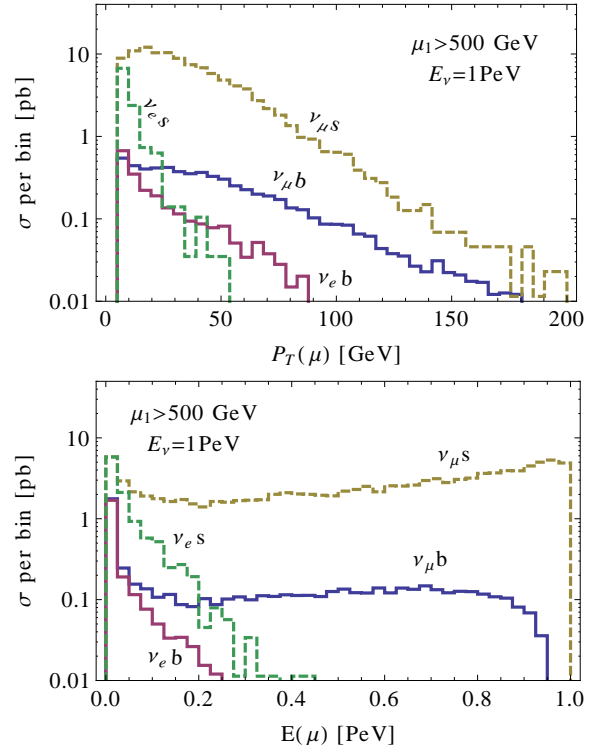


FIG. 4: Muon  $P_T$  and energy distributions for incoming neutrino energy at 1 PeV. The labels of the curves denote the type of neutrino and the target sea-type quark. The highest energy muon in an event is required to have energy greater than 0.5 PeV.

The angular separation between  $\mu_1$  and  $\mu_2$  is typically small, due to the high Lorentz boosts, yet some events will have an angular separation as large as 1 deg, as shown in Fig 5. The  $\mu_2$  from top production is more likely to lead to a larger angular di-muon separation than is the case for charm. When the two muons originate in the rock or ice prior to reaching the detector, the spatial separation of their tracks within the detection may be resolved. A full detector simulation is necessary to properly judge the ability of IceCube to distinguish the tracks of the two muons. Also, tri-muon events can arise from  $\nu_\mu$  production of the top quark and its decays to  $W$  plus a  $b$ -quark (9 percent probability), with a primary muon from the neutrino vertex, a muon from leptonic  $W$ -decay and the third muon from  $B$ -decay; such an event is rare

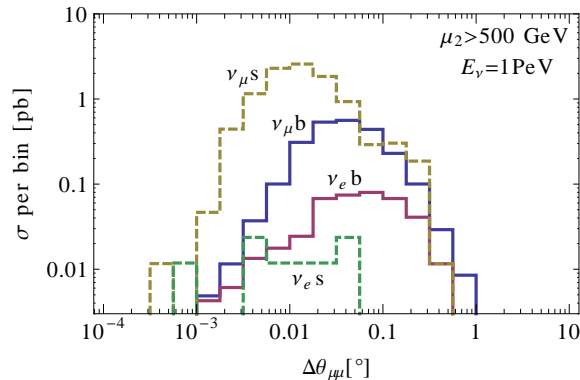


FIG. 5: Angular separation between the leading dimuons. An energy requirement of 500 GeV is imposed on the second most energetic muon ( $\mu_2$ ). Each curve is normalized to the fraction of the scattering cross-section that yields at least two muons with a  $\mu_2$  energy above 500 GeV. Colors and labels are the same as in Fig. 4

(of order  $10^{-3}$ ) but background free. Serendipitous discovery of the tri-lepton signature is possible if close-by muon tracks can be distinguished.

## V. SUMMARY

Weak production of the top-quark gives an increase of order 5 percent in the neutrino deep inelastic scattering cross section at PeV energies, with a sharp threshold rise. Single charm production contributes about 25 percent. With semi-leptonic decays, both give rise to dimuon events with distinctive kinematic characteristics. The tracks of the two muons may be separated by up to one degree in the IceCube detector. The top quark gives a unique and background free, but rare, three muon signal. The discovery of energetic multi-muon events by IceCube will be a physics tour de force of great interest.

## VI. ACKNOWLEDGEMENTS

VB thanks Fred Olness for illuminating discussions about the  $b$ -quark PDF. This work is partially supported by the U.S. Department of Energy under grants DE-AC02-06CH11357 and DE-FG-02-12ER41811. YG thanks the Mitchell Institute for Fundamental Physics and Astronomy (MIFPA) and Wayne State University for support.

- 
- [1] R. Gandhi, C. Quigg, M.H. Reno and I. Sarcevic, arXiv:hep-ph/9512364; C.A. Argüelles, F. Halzen, L. Wille, M. Kroll and M.H. Reno, arXiv:1504.06639; L.A. Anchordoqui, M.M. Block, L. Durand, P. Ha, J.F. Soriano and T. Weiler, arXiv:1611.07905; I.F.M. Albuquerque, G. Burdman and Z. Chacko, arXiv:hep-ph/0605120.
- [2] C. Quigg, M.H. Reno, and T.P. Walker, Phys. Rev. Lett. **57**, 6 (1986); A. Cooper-Sarkar and S. Sarkar, arXiv:0710.5303; A. Cooper-Sarkar, P. Mertsch and S. Sarkar, arXiv:1106.3723.
- [3] M. G. Aartsen *et al.* [IceCube Collaboration] arXiv:1609.04981; also see arXiv:1710.03731 and references therein to earlier data and analyses of the IceCube Collaboration.
- [4] L. A. Anchordoqui *et al.* JHEAp 1-2 (2014) 1-30 arXiv:1312.6587 [astro-ph.HE]
- [5] M. G. Aartsen *et al.* [IceCube Collaboration], arXiv:1607.05886 [astro-ph.HE].
- [6] V. Barger and W.-Y. Keung, Phys. Lett. B **727**, 190 (2013) [arXiv:1305.6907 [hep-ph]].
- [7] B. Dutta, Y. Gao, T. Li, C. Rott and L. E. Strigari, Phys. Rev. D **91**, 125015 (2015) [arXiv:1505.00028 [hep-ph]].
- [8] U. K. Dey and S. Mohanty, JHEP **1604**, 187 (2016) [arXiv:1505.01037 [hep-ph]].
- [9] B. Feldstein, A. Kusenko, S. Matsumoto and T. T. Yanagida, Phys. Rev. D **88**, no. 1, 015004 (2013) [arXiv:1303.7320 [hep-ph]].
- [10] Y. Bai, R. Lu, and J. Salvado, JHEP **1601** (2016) 161 [arXiv:1311.5864]
- [11] L. A. Anchordoqui, V. Barger, H. Goldberg, X. Huang, D. Marfatia, L. H. M. da Silva and T. J. Weiler, Phys. Rev. D **92**, no. 6, 061301 (2015) Erratum: [Phys. Rev. D **94**, no. 6, 069901 (2016)], [arXiv:1506.08788 [hep-ph]].
- [12] M. Ahlers, Y. Bai, V. Barger and R. Lu, Phys.Rev. D **93** (2016) no.1, 013009, arXiv:1505.03156 [hep-ph]
- [13] A. Bhattacharya, R. Enberg, Y. S. Jeong, C. S. Kim, M. H. Reno, I. Sarcevic and A. Stasto, arXiv:1607.00193 [hep-ph].
- [14] F. Halzen and L. Wille, Phys. Rev. D **94**, no. 1, 014014 (2016) [arXiv:1605.01409 [hep-ph]].
- [15] R. Gauld, J. Rojo, L. Rottoli and J. Talbert, JHEP **1511**, 009 (2015) [arXiv:1506.08025 [hep-ph]].
- [16] R. Laha and S. J. Brodsky, arXiv:1607.08240 [hep-ph].
- [17] E. Waxman and J. N. Bahcall, Phys. Rev. D **59**, 023002 (1999) [hep-ph/9807282].
- [18] S. Dulat, T.J. Hou, J. Gao, M. Guzzi, J. Huston, P. Nadolsky, J. Pumplin, C. Schmidt, D. Stump, and C.P. Yuan, EPJ Web Conf. 120 (2016) 07003
- [19] D. Clark, E. Godat and F. Olness, [arXiv:1605.08012 [hep-ph]]
- [20] R. V. Harlander and W. B. Kilgore, Phys. Rev. D **68**, 013001 (2003) [hep-ph/0304035]
- [21] F. Maltoni, Z. Sullivan and S. Willenbrock, Phys. Rev. D **67**, 093005 (2003) [hep-ph/0301033].
- [22] B. A. Dobrescu and R. K. Ellis, Phys. Rev. D **69**, 114014 (2004) [hep-ph/0310154]
- [23] J. Alwall *et al.*, JHEP **1407**, 079 (2014) [arXiv:1405.0301 [hep-ph]].
- [24] T. Sjostrand, S. Mrenna and P. Z. Skands, JHEP **0605**, 026 (2006) doi:10.1088/1126-6708/2006/05/026 [hep-ph/0603175].